Final Report

KAUST Academy - ICTP

Project

Digital Holography Microscope (DHM) for Automatic Disease Identification Using AI

Group Members

Jana Zakai
Software Engineering
University of Jeddah

Maher Alhejaili
Computer Science
University of Tabiah

Project Mentor

Dr. Humberto Cabrera

Dr. Luis Garcia Ordoñez

Mr. Antonio Bassi

1. Overview

This report summarizes the progress and findings of the research project on Digital Holography Microscopy (DHM) for automated disease identification using artificial intelligence applications.

Blood-related diseases such as malaria, sickle cell anemia, and thalassemia affect millions globally, particularly in resource-limited regions. According to the World Health Organization (2023), malaria alone caused over 600,000 deaths in 2022, with the highest burden in sub-Saharan Africa. Accurate diagnosis is critical but often relies on manual microscopic examination of stained blood smears — a process that is time-consuming, requires trained personnel, and is prone to inter-operator variability [5].

Sickle cell anemia and thalassemia also require specialized diagnostic techniques (e.g., hemoglobin electrophoresis, molecular testing), which are often unavailable in rural clinics due to high cost and lack of infrastructure [6].

These limitations highlight the need for a portable, rapid, and low-cost diagnostic alternative that works without staining, is automated, and can be deployed at the point-of-care, especially in low-income settings.

2. Research Aim

This research aims to enhance design, develop, and validate a compact, field-deployable Digital Holographic Microscopy (DHM) system integrated with machine learning algorithms for the automated, label-free detection of malaria, sickle cell anemia, and thalassemia.

By leveraging the quantitative phase imaging (QPI) capabilities of DHM, which capture cellular morphology and refractive index variations, and applying deep learning models, the system will enable real-time, cost-effective, and high-accuracy disease classification. The proposed solution aligns with global health priorities to expand access to diagnostics and improve outcomes in underserved regions.

3. Project Timeline

Phases	Description
Literature Review and project introduction	Papers on DHM
	FPGA Courses and Lab work
Lab Experimentation	Parameter Testing
	Optimal image capturing
	Morphological Data Analysis
Denoising Algorithm	Dataset preparation
	Architecture Design
	Implementation & Testing
Raspberry Pi Migration	Convert code into raspberry Pi compatible
	Integrate motor control and image acquisition systems
AI classification Algorithm	Dataset Preparation
	Architecture Design
	Implementation & Testing

4. Background Research

4.1. On-Axis Digital Holographic Microscopy: Current Trends and Algorithms

On-axis digital holographic microscopy (DHM) offers a robust and label-free imaging modality capable of capturing both amplitude and phase information from transparent or semi-transparent samples. This capability is particularly advantageous in biomedical imaging, where staining may be undesirable or infeasible.

Reconstruction algorithms in on-axis DHM are generally categorized into three main approaches: direct, iterative, and machine learning-based. Direct methods such as angular spectrum propagation are computationally efficient and easy to implement but are prone to image artifacts, including the twin-image effect, due to the lack of phase diversity. Iterative methods address these issues by minimizing a cost function across multiple reconstruction steps and often incorporate regularization constraints, such as total variation minimization or sparsity. Although they offer improved reconstruction accuracy, iterative techniques are computationally intensive. Recent advances in computational power and algorithmic design have made such methods more feasible for real-time applications. Machine learning-based approaches, particularly those employing convolutional neural networks or learned sparsifying transforms, allow for high-quality reconstructions in a single inference pass. These methods offer speed and robustness but require extensive annotated datasets and significant training resources. A unified nomenclature and comparative benchmarks of various reconstruction strategies have been proposed to facilitate method selection. In biomedical applications such as disease diagnosis, these methods enhance the clarity and interpretability of morphological features essential for identifying conditions like malaria, sickle cell anemia, and thalassemia **[1]**.

4.2. Wide Field-of-View Common-Path Lateral-Shearing Digital Holographic Interference Microscope

This study presents the development of a common-path digital holographic microscope employing a lateral-shearing geometry. The microscope is designed to improve the temporal stability and portability of traditional two-beam Mach–Zehnder-based digital holographic interference microscopes (MZ-DHIM), which, although capable of high-resolution 3D imaging, suffer from low temporal stability due to their reliance on two separate optical paths. These setups also involve multiple optical components, making them bulky and expensive.

To address these limitations, the authors implement a common-path geometry where the object wavefront is duplicated, and one of the wavefronts is filtered through a pinhole to generate a separate reference beam. This design maintains the simplicity of self-referencing setups while significantly expanding the field of view—achieving a coverage comparable to two-beam systems. The implementation uses a 635 nm laser diode, a 40× microscope objective, a glass shearing plate, and a 30 μm pinhole to filter the reference beam. Both CCD and webcam sensors are used to capture holograms, demonstrating the system's flexibility and cost-efficiency.

Image reconstruction is performed using angular spectrum propagation, allowing effective separation of diffracted components and enabling accurate phase retrieval without the need for propagation when the detector plane coincides with the image plane. The microscope achieves subnanometer temporal stability—0.81 nm for the CCD-based system and 0.94 nm for the webcam-based system—making it suitable for detecting red blood cell thickness fluctuations in the nanometer range. Experimental validation using polystyrene microspheres confirmed its 3D imaging accuracy, and subsequent measurements of red blood cell morphology and membrane dynamics further demonstrated its biomedical potential **[2]**.

4.3. Highly Stable Digital Holographic Microscope Using Sagnac Interferometer

In this work, Mahajan et al. introduce a compact and highly stable digital holographic microscope based on Sagnac interferometer geometry as described in **figure 1**. This configuration ensures that both object and reference beams propagate through identical optical elements, but in opposite directions, thus significantly enhancing temporal stability without requiring vibration isolation.

The system employs a 532 nm diode laser, a 40× objective lens, and a collimating lens to generate a coherent beam. The beam is split using a non-polarizing cube beamsplitter and directed into a closed-loop path by mirrors, creating an off-axis configuration. At the Fourier plane of the imaging optics, a pinhole spatially filters one beam to generate a clean reference wavefront, while the second beam serves as the object wavefront. Reconstruction is carried out using angular spectrum propagation, enabling numerical focusing and accurate thickness measurement.

Temporal stability measurements demonstrate the system's robustness: the CCD-based implementation achieves 0.54 nm stability, while the webcam-based version achieves 0.72 nm, both without any vibration isolation. These stability values are significantly better than those of traditional Mach–Zehnder-based systems, even when the latter employ isolation mechanisms. The microscope effectively captures red blood cell membrane oscillations, with the extracted fluctuation profiles and frequency distributions confirming its capability to resolve dynamic cellular behavior in the tens-of-nanometers range.

The use of a webcam sensor offers a cost-effective alternative to CCDs, making the system more accessible for point-of-care diagnostics. Unlike self-referencing methods, the Sagnac geometry offers a fully usable field of view and higher phase reconstruction quality. Consequently, this setup combines simplicity, high stability, and affordability, enabling label-free monitoring of biophysical changes in cells and opening avenues for disease detection based on cellular dynamics **[3]**.

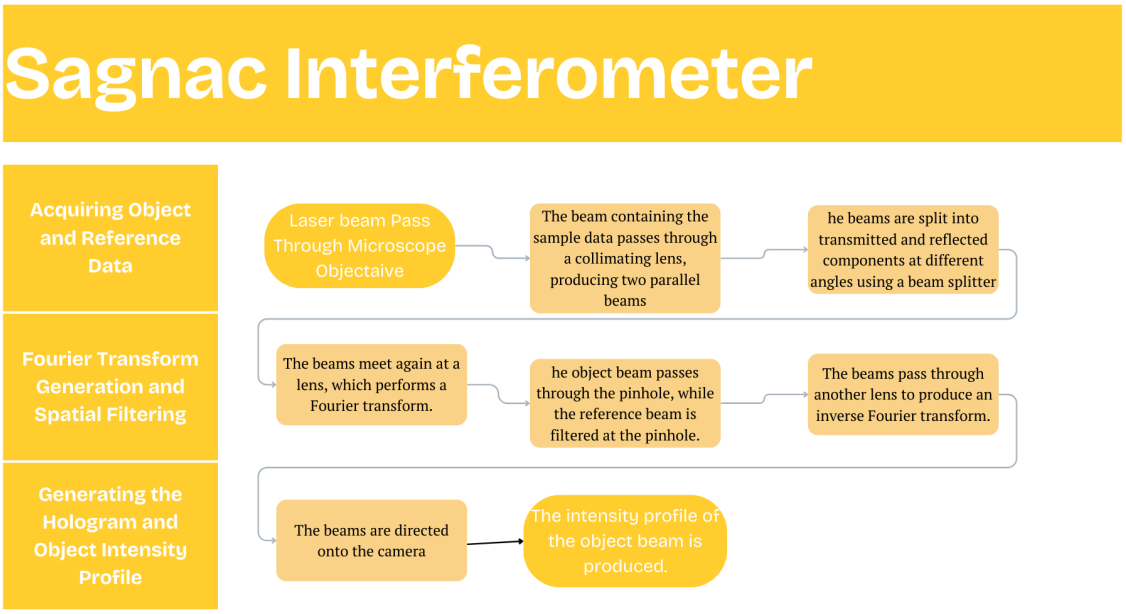

Figure 1 Sagnac interferometer geometry

5. Methodology

The proposed system enhancement process is structured across three primary domains, each comprising several sequential phases. These domains—optical system deployment, digital infrastructure enhancement, and AI algorithm integration—are interdependent and collectively aim to improve the stability, portability, and diagnostic power of the digital holographic microscopy platform.

5.1 Deployment of the Sagnac Setup

This domain involves the physical construction and validation of the DHM system using a Sagnac interferometer geometry, chosen for its inherent temporal stability and compactness.

5.1.1 Structural and Physical Architecture

The Sagnac-based DHM system is assembled using a diode laser module, beam-splitting optics, spatial filtering via a pinhole, and imaging sensors (CCD and/or CMOS webcam). The optical layout ensures that both object and reference beams traverse the same optical components in opposite directions, minimizing environmental phase noise and mechanical vibrations.

5.1.2 Testing and Calibration

The system is calibrated using polystyrene microspheres of known diameter to validate the accuracy of phase reconstruction and 3D imaging. Phase stability is evaluated by recording holograms over time with a blank sample,

computing both spatial and temporal standard deviations. These metrics establish the system's suitability for imaging nanometric-scale cellular fluctuations.

5.1.3 Analysis

Quantitative phase and optical thickness profiles of biological samples, such as red blood cells, are extracted. Both static and dynamic parameters—including membrane fluctuations, projected area, and optical volume—are analyzed to confirm the microscope's diagnostic viability.

5.2 DHM Software and Hardware Enhancement

This component focuses on upgrading the digital pipeline and hardware environment of the DHM system to improve performance, portability, and maintainability.

5.2.1 Code Refactoring and Enhancement

Legacy code used for hologram reconstruction and visualization is modularized and optimized for speed, clarity, and scalability. The reconstruction process is refined to support compact processing.

5.2.2 Hardware Migration

The processing and acquisition pipeline is migrated from high-end laboratory computers to compact, edge-compatible platforms, specifically Raspberry Pi. This ensures low power consumption and facilitates deployment in field or point-of-care environments.

5.3 AI Algorithm Deployment

The final domain introduces machine learning models into the DHM pipeline to enhance image quality and enable automated sample classification.

5.3.1 Cells segmentation

A Deep learning model using SAM architecture is trained to perform segmentation of blood cells using phase images, targeting issues such as speckle noise and phase aberrations. This improves the interpretability of morphological features and allows users to choose which cells to process.

5.3.2 Dataset Collection and Annotation

A domain-specific dataset comprising phase images and corresponding labels is curated. Both synthetic and experimentally acquired data are used to augment the dataset.

5.3.3 Model Architecture and Training

Convolutional neural networks (CNNs) or transformer-based architectures are developed to classify cell types or detect anomalies based on their phase signatures. The models are trained using the collected dataset and evaluated

for classification accuracy, sensitivity, and specificity.

5.3.4 Deployment and Testing

The trained models are integrated into the DHM system, enabling real-time classification and feedback during hologram acquisition. The performance of the AI-enhanced pipeline is benchmarked against manual annotations and conventional image processing results.

6. System Design

6.1. System Pipeline

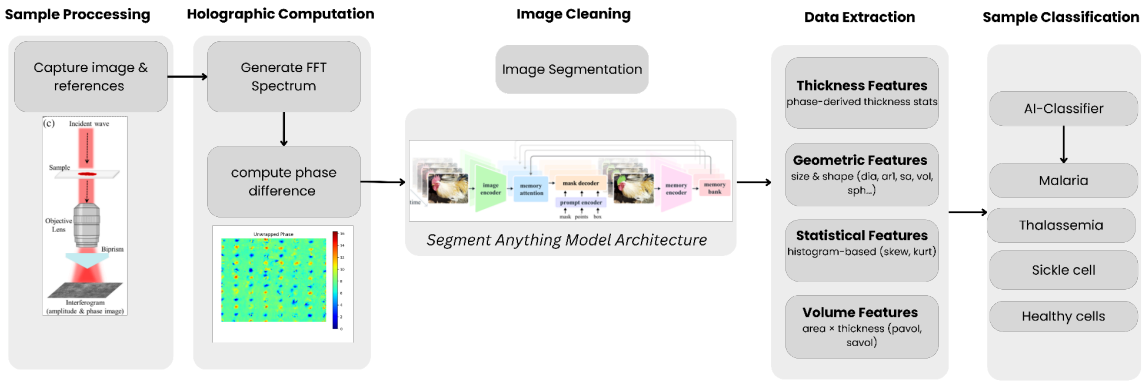

Figure 2 System Pipeline

The prior version of the DHM was designed to include sample processing by which the image is captured by the digital camera and passed to the software that performs holographic computations and then extract the profile data.

This enhanced DHM works with the illustrated pipeline in **figure 2** introducing AI image cleaning after performing holographic computations and AI classification after data extraction.

6.2 System Architecture

The system architecture was changed from a 1-tier architecture to a new 2-tier architecture as illustrated in **figure 3**, allowing us to introduce remote control to the system.

- **1-tier local architecture:** Both client and backend run on the same machine, which simplifies deployment but limits scalability.
- **2-tier remote architecture:** The client side (HTML/CSS, App.js) communicates with a remote server (Server.js) over the network. This approach improves modularity, allows remote access, and separates the presentation from the logic layer.

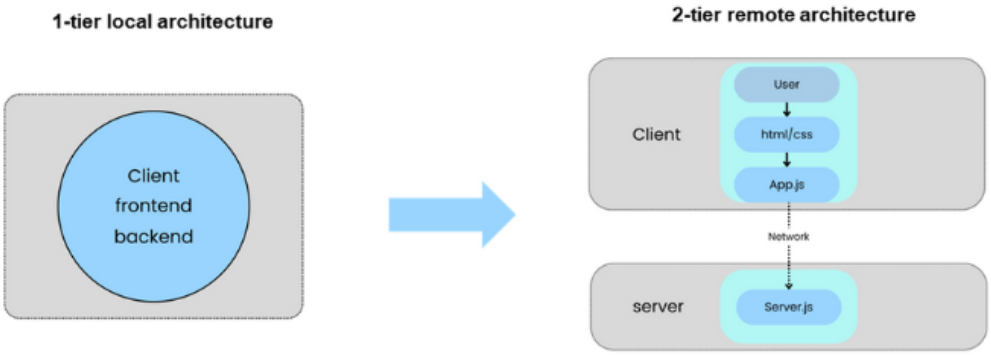

Figure 3 Comparison between 1-tier local architecture and 2-tier remote architecture.

6.3 Internal Data Flow

The following sequence diagram **(figure 4)** illustrates the interaction between the user, front-end, and back-end modules and how the data is transferred between these system modules, specifically representing one use case of requesting a 1D-profile from the system.

The user initiates a request for a 1D profile, which flows through the web interface (index.html and App.js), then to the server (Server.py), and finally to the system functions module (Sys_functions.py) for computation. The results (distance and thickness values) are then returned and visualized for the user.

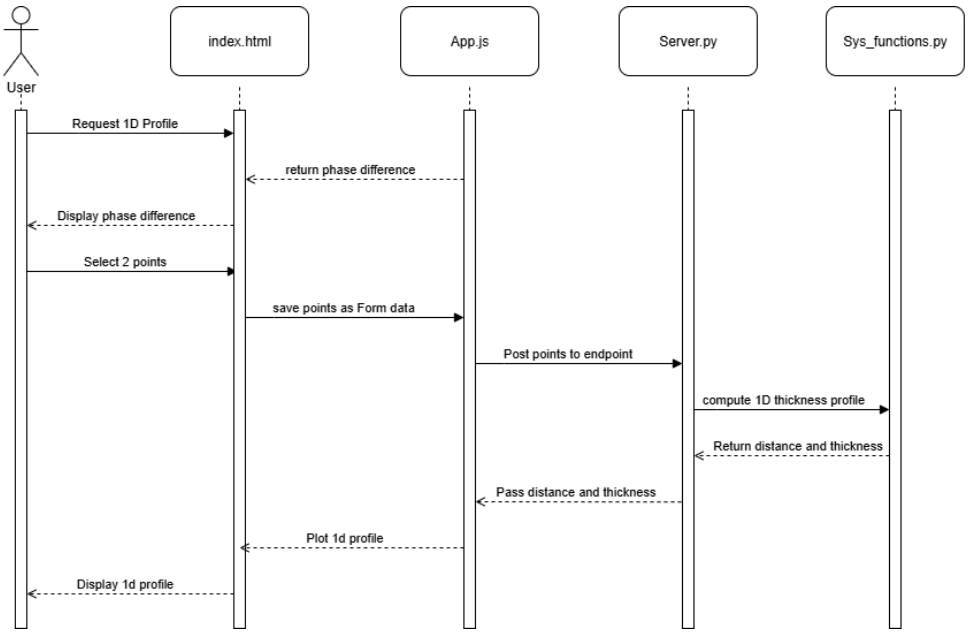

Figure 4 Sequence diagram showing the process of requesting and computing a 1D profile.

7. Results

7.1. Cells segmentation results

For cleaning the phase difference image (PSI) after computation, several methods were deployed during experimentation. The preliminary method that was used in the prior version of the DHM was cleaning with Mean-level thresholding as shown in **Figure 5**. However, this way removes information that is useful for the data extraction.

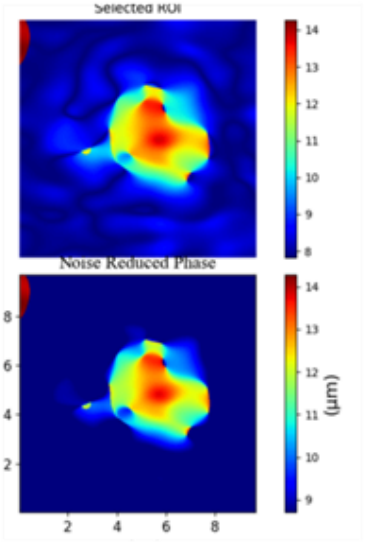

Figure 5 Mean-Level Thresholding Result

The output that is desired is a segmentation of the image and not a denoised image. Thus, a pretrained model, Segment Anything Model (SAM) developed by Meta [4], was utilised to segment the PSI in a way that the cell structure is not altered.

The following images, **figure 6** and **figure 7,** are some tests we conducted on blood cells images taken in the past couple of weeks. The segmentation model yielded accurate results so far but still needs integration into the software. Such accurate segmentation results omit the need of a denoising model.

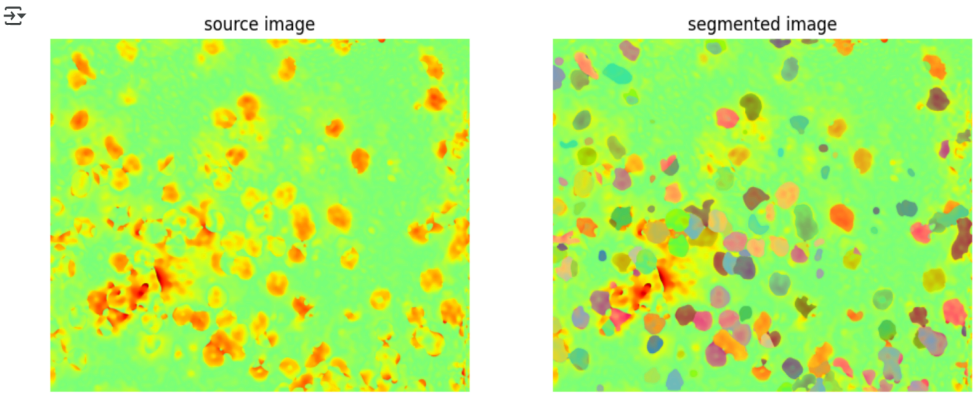

Figure 6 Segmentation result

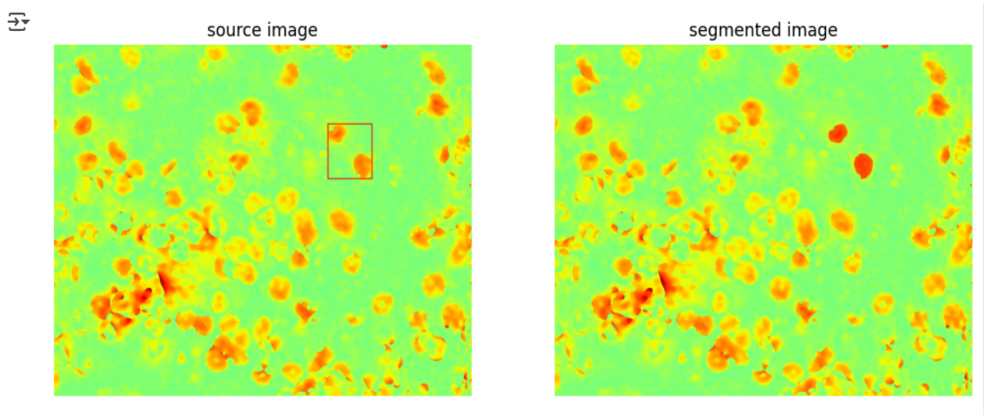

Figure 7 Blood-cells detection result

7.2. AI Classification Results

17 quantitative features were extracted out of healthy and Malaria infected blood sample, forming a dataset of 215 healthy cells and 252 malaria cells data entries, which was used for training the AI classifiers, representing different categories of RBC morphology and internal structure:

- **Geometric and Shape Features**: Diameter (dia), aspect ratio (ar1), projected area (pa), surface area (sa), volume (vol), sphericity (sph), and sphericity corrected by refractive index (sph_with_ri). These features quantify the overall shape, size, and deformability of RBCs, which are often altered in malaria infection due to parasite-induced swelling and changes in cell membrane rigidity.

- **Thickness and Optical Features**: Mean thickness (th), maximum thickness (max_thick), average thickness (mean_thick), thickness variability (std_thick), and relative variation (cv_thick). These were extracted directly from phase maps, where pixel intensity corresponds to cell optical path length. Malaria-infected cells typically display greater heterogeneity and localized thickening due to the presence of intraerythrocytic parasites.

- **Statistical Texture Features**: Skewness (skew) and kurtosis (kurt) of the thickness distribution. These higher-order statistical measures describe irregularities in pixel intensity profiles, capturing asymmetry and extreme deviations introduced by parasite inclusions.

- **Volume-Related Features**: Projected volume (pavol) and surface-area volume (savol), which combine cell area with average thickness to approximate three-dimensional structure. These measures highlight the swelling and morphological distortions that are characteristic of infected RBCs.

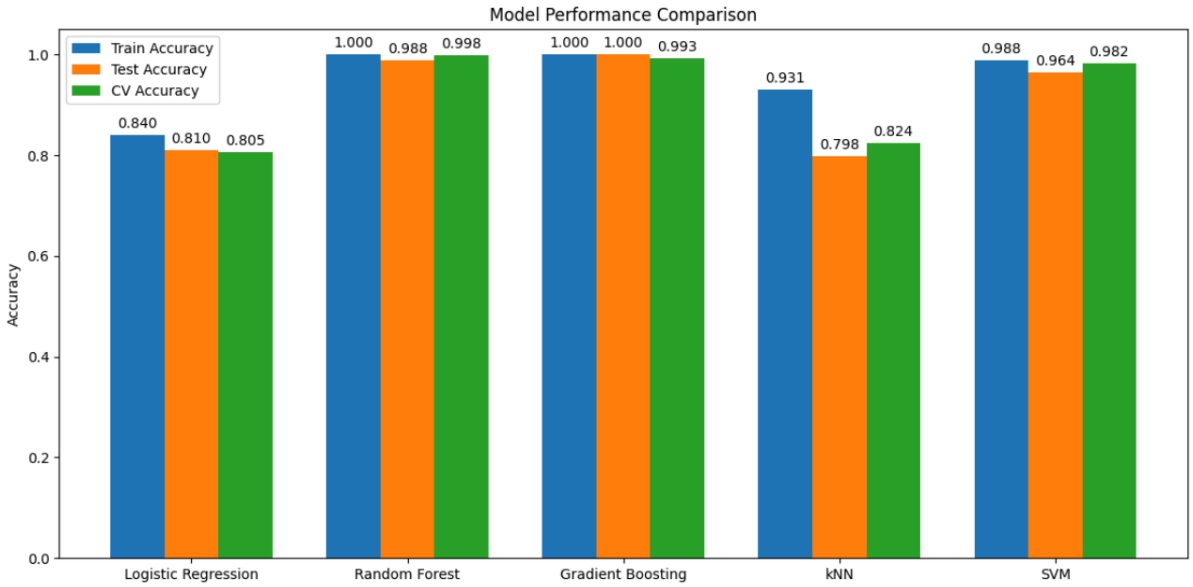

Figure 8 Model Performance Comparison

Utilising the dataset, we trained a classifier on 5 different models showcasing their performance in **figure 8**. The mean value was used to counter the missing data entries. Tree based models, Gradient boosting and Random Forest, resulted in a high performance due to overfitting which is undesired. On the other hand, the Support Vector Machine (SVM) model presents the highest performance with a cross validation accuracy of 98%.

7.3. Remote Setup and Server Integration

To enable distributed processing and remote computation of Digital Holographic Microscopy (DHM) data, we integrated the frontend, backend, and remote server as follows:

7.3.1. Frontend to Server Communication

The existing graphical user interface (GUI) was modified to collect all required parameters (wavelength, pixel size, magnification, RI difference, DC removal, filter type, filter size, beam type, and noise threshold).

Parameters were serialized to JSON format and sent via HTTP POST requests to the server using the requests library.

Images and reference files were prepared for transfer via SCP protocol for remote storage and processing.

7.3.2. Server Setup Using FastAPI

A lightweight server was developed using FastAPI to handle incoming parameter requests and trigger backend computation.

Endpoints were created for:

1. /set_params → receiving JSON parameters and updating internal backend state.

2. /run_phase_difference → executing the phase unwrapping computation using remotely uploaded images.

Error handling and validation were implemented using Pydantic models, ensuring type-safe parameter handling.

7.3.3. Backend Integration

The backend (core image processing and DHM phase unwrapping code) was refactored to accept input parameters and image file paths dynamically.
Helper functions were added to parse parameters, convert types, and update backend variables seamlessly from remote input.

7.3.4. Remote File Handling

Images were transferred to the remote machine using SCP and placed in the processing directory. The backend processed these files and returned computed results (unwrapped phase image) to the server, which were then sent back to the frontend for visualization.

7.3.5. Remote UI

A complete new user interface, as shown in **Figure 9**, was developed for the remote setup, using HTML, CSS, and javascript. This new way of showing the graphical user interface will guarantee the frontend can work flawlessly on any operating system and will also insure the number of dependencies is limited

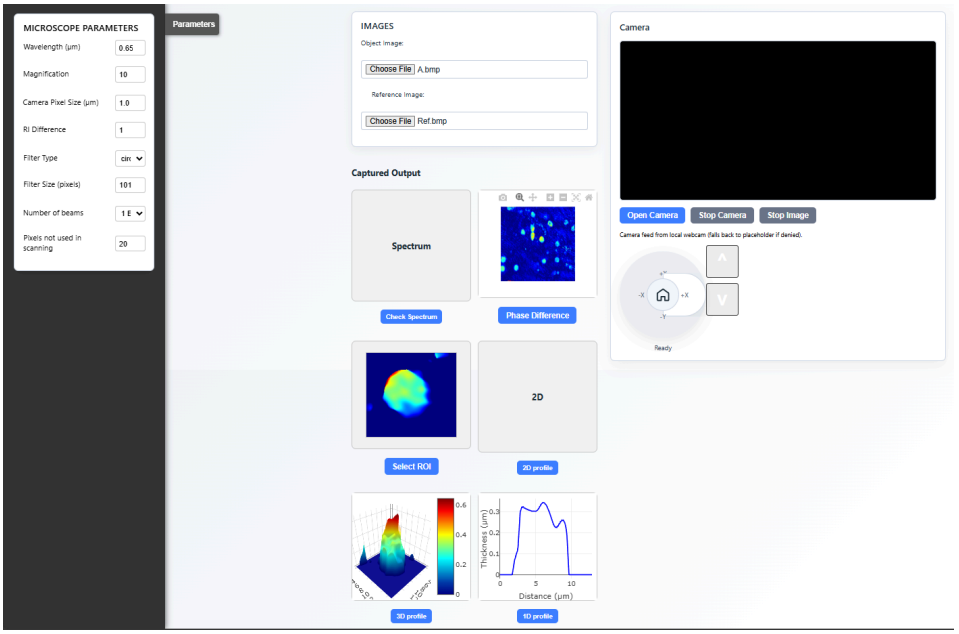

Figure 9 Showcasing new user interface designed for the remote control setup

7.3.6. Remote motor control

After assembling the hardware components onto the Raspberry Pi platform, we successfully integrated GPIO-based motor control for automated sample stage movement. The code was extended to support directional movement commands from the frontend interface, allowing users to reposition the microscope slide remotely. This provides an essential step toward fully remote-operated DHM experiments, particularly valuable for field deployments or telemedicine applications.

8. Challenges

Throughout the development of the DHM system, several challenges were encountered across both hardware and software domains. Aligning the Sagnac interferometer with sufficient precision required iterative adjustments and careful optical calibration to achieve the desired phase stability. The use of low-cost imaging sensors such as webcams introduced limitations in dynamic range and sensitivity, necessitating additional image enhancement techniques.

On the software side, integrating the AI segmentation model into the real-time DHM pipeline proved complex due to variations in image resolution, noise artifacts, and inconsistencies in sample preparation. Moreover, establishing stable and secure communication between the frontend, backend, and remote server using SCP and FastAPI required careful management of file paths, error handling, and parameter serialization.

9. Future work

Potential works will focus on expanding the clinical scope of the DHM system by exploring its application in the classification of Thalassemia and Iron Deficiency Anemia. By leveraging morphological phase features and advanced AI models, the system can potentially differentiate between these conditions based on blood cell characteristics. Additionally, further testing and calibration of the Sagnac setup will be conducted to ensure optimal performance under varying conditions and sample types, thereby increasing robustness and repeatability. Integration of the AI-based cell segmentation model into the full DHM pipeline remains a priority, allowing seamless automation from image acquisition to classification. Enhancing the graphical user interface to support higher resolution outputs will also improve user experience and diagnostic clarity.

10. Conclusion

This report presents the successful deployment of a Digital Holography Microscope integrated with AI-driven segmentation and remote control capabilities. The modular system architecture—comprising optical setup, AI pipeline, and web-based interface—has demonstrated promising results in stable phase acquisition and preliminary classification of blood cells. The integration of a FastAPI backend and SCP-based image transfer enables real-time remote interaction, paving the way for accessible point-of-care diagnostics. With future work focusing on expanded disease classification, tighter pipeline integration, and improved usability, this project stands poised to contribute meaningfully to biomedical imaging and global health diagnostics.

11. References

[1] S. A. Alhichri, M. A. Siddiqui, and S. M. Munir, "On-axis digital holographic microscopy: Current trends and algorithms," *Optics and Laser Technology*, vol. 163, p. 109395, May 2023, doi: 10.1016/j.optlastec.2023.109395.

[2] P. Vora, V. Trivedi, S. Mahajan, N. Patel, M. Joglekar, V. Chhaniwal, A.-R. Moradi, B. Javidi, and A. Anand, "Wide field of view common-path lateral-shearing digital holographic interference microscope," *Journal of Biomedical Optics*, vol. 22, no. 12, p. 126001, Dec. 2017, doi: 10.1117/1.JBO.22.12.126001.

[3] S. Mahajan, V. Trivedi, P. Vora, V. Chhaniwal, B. Javidi, and A. Anand, "Highly stable digital holographic microscope using Sagnac interferometer," *Optics Letters*, vol. 40, no. 16, pp. 3743–3746, Aug. 2015, doi: 10.1364/OL.40.003743.

[4] Meta AI Research, “Segment Anything,” GitHub repository, 2023. [Online]. Available: https://github.com/facebookresearch/segment-anything

[5] The Guardian, “Global malaria deaths rise due to drug and insecticide resistance, climate crisis, and funding gaps,” Dec. 11, 2024. [Online]. Available: https://www.theguardian.com/global-development/2024/dec/11/global-health-deaths-malaria-rise-drug-insecticide-resistance-climate-crisis-funding-un

[6] The Guardian, “Antibiotic-resistant bacterial infections complicate malaria diagnosis and increase coma mortality,” Jul. 3, 2025. [Online]. Available:

https://www.theguardian.com/global-development/2025/jul/03/antibiotics-children-coma-africa-malaria-bacterial-infection-research

[7] S. Alsaeed, et al., “Prevalence of sickle cell trait and disease in Saudi Arabia: A cross-sectional analysis,” Saudi Journal of Hematology, vol. 12, no. 4, pp. 201–208, 2024. [Online]. Available: https://pmc.ncbi.nlm.nih.gov/articles/PMC12111217/

[8] H. Almalki, et al., “β-thalassemia carrier prevalence in Saudi Arabia and implications for premarital screening,” Human Genomics, vol. 18, no. 1, pp. 54–63, Mar. 2024. [Online]. Available: https://link.springer.com/article/10.1007/s44197-024-00281-x

[9] Ministry of Health, Saudi Arabia, “Premarital Screening Program,” MOH, Riyadh, Saudi Arabia, 2024. [Online]. Available: https://www.moh.gov.sa/